

PAPER • OPEN ACCESS

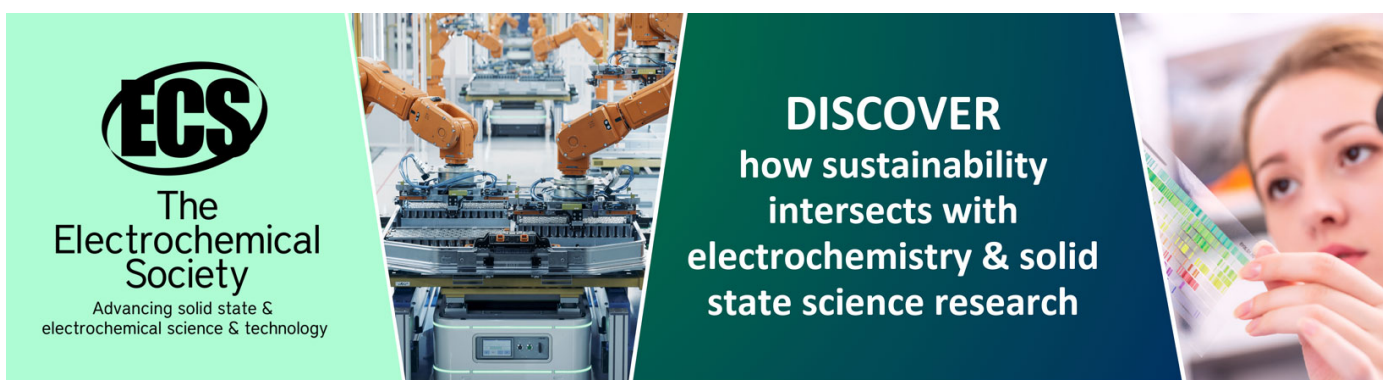
Generation of sub-gigabar-pressure shocks by a hyper-velocity impact in the collider driven by laser-induced cavity pressure

To cite this article: J Badziak *et al* 2018 *J. Phys.: Conf. Ser.* **959** 012012

View the [article online](#) for updates and enhancements.

You may also like

- [The National Direct-Drive Inertial Confinement Fusion Program](#)
S.P. Regan, V.N. Goncharov, T.C. Sangster *et al.*
- [Glass Frit Wafer Bonding - Sealed Cavity Pressure in Relation to Bonding Process Parameters](#)
Roy Knechtel, Sophia Dempwolf and Holger Klingner
- [Experimental measurements of the cavitating flow after horizontal water entry](#)
Thang Tat Nguyen, Duong Ngoc Hai, Nguyen Quang Thai *et al.*



ECS
The
Electrochemical
Society
Advancing solid state &
electrochemical science & technology

DISCOVER
how sustainability
intersects with
electrochemistry & solid
state science research

Generation of sub-gigabar-pressure shocks by a hyper-velocity impact in the collider driven by laser-induced cavity pressure

J Badziak¹, M Kucharik², R Liska²

¹Institute of Plasma Physics and Laser Microfusion, 01-497 Warsaw, Poland

²Czech Technical University, FNSPE, 160 41 Prague 6, Czech Republik

E-mail: jan.badziak@ifpilm.pl

Abstract. The generation of high-pressure shocks in the newly proposed collider in which the projectile impacting a solid target is driven by the laser-induced cavity pressure acceleration (LICPA) mechanism is investigated using two-dimensional hydrodynamic simulations. The dependence of parameters of the shock generated in the target by the impact of a gold projectile on the impacted target material and the laser driver energy is examined. It is found that both in case of low-density (CH, Al) and high-density (Au, Cu) solid targets the shock pressures in the sub-Gbar range can be produced in the LICPA-driven collider with the laser energy of only a few hundreds of joules, and the laser-to-shock energy conversion efficiency can reach values of 10 – 20 %, by an order of magnitude higher than the conversion efficiencies achieved with other laser-based methods used so far.

1. Introduction

The production of high dynamic pressures using shock waves is a hot topic developed in various branches of research, in particular in high energy-density physics (HEDP) [1], material science [2,3] or inertial confinement fusion (ICF) [4]. The pressures in the multi-Mbar range can be achieved by a large variety of methods employing chemical [5] or nuclear explosions [6], irradiation of a solid target by the laser beam [4,7-10] or the laser-produced X-rays [4,11] as well as the hyper-velocity impact, into a dense target, of a projectile accelerated by a pulsed-power machine [12], a light-gas gun [2,13] or a laser driver [14-19]. However, the pressures in the sub-Gbar or Gbar range are attainable only with laser-based methods or the nuclear explosions (which are forbidden presently). A common drawback of all laser-based methods of the shock generation used so far is the low efficiency of energy conversion from a laser to the shock, $\eta_{is} = E_s/E_L$, which is below a few percent [4,9,15,18] (E_s is the shock energy and E_L is the energy of a laser beam which generates the shock or produces X-rays or accelerates the projectile). In case of the shock generation by the laser-driven hyper-velocity impact, the main reason for the low η_{is} value is the low energetic efficiency of projectile acceleration in the commonly used ablative acceleration (AA) scheme, which is $\eta_{acc} = E_p/E_L \sim 0.5 - 5\%$ [15-19] (E_p is the projectile kinetic energy). As a result, for the generation of sub-Gbar or Gbar shocks of spatial dimensions enabling their practical usefulness (e.g. studies of equations of state of materials), multi-kJ laser drivers are necessary [15]. Recently, a novel efficient scheme of generation of high-pressure shocks - called the LICPA-driven collider - has been proposed [20,21] (LICPA - laser-induced cavity pressure acceleration [22,23]). In the collider, a projectile (e.g. a heavy disc covered by a low-Z ablator) placed in a cavity is irradiated by a laser beam introduced into the cavity through a hole and



then accelerated in a cylindrical or conical guiding channel by the pressure created in the cavity by the laser-produced hot plasma expanding from the irradiated side of the projectile or by the photon (radiation) pressure of the ultra-intense laser pulse trapped in the cavity. The projectile accelerated in the channel impacts into a dense target placed at the channel exit. Due to the impact, the projectile energy and momentum are rapidly transferred to the target and when the projectile velocity significantly surpasses the sound velocity in the target, a high-pressure shock is generated in the target. It has been demonstrated [20,21] that using the LICPA-driven collider, a high-pressure shock can be generated in a solid target with the laser beam energy much lower than that required for producing such a shock with other laser-based methods used so far.

In this paper, the process of shock generation in the LICPA-driven collider is investigated with the use of numerical hydrodynamic simulations. A particular attention is paid to the dependence of shock parameters and the laser-to-shock energy conversion efficiency on the impacted target material and the laser driver energy. It is shown that both in case of low-density (CH, Al) and high-density (Cu, Au) solid targets the shock pressure in the sub-Gbar range can be generated in the target with the laser driver energy of only a few hundreds of joules and the laser-to-shock energy conversion efficiency can reach values above 10 %.

2. Results of numerical simulations

For numerical investigations of shock generation by a hyper-velocity impact in the LICPA-driven collider we used the two-dimensional (2D) hydrodynamic PALE (Prague Arbitrary Lagrangian Eulerian) code [24,25]. The numerical simulations comprised both the projectile acceleration phase and the phase of the projectile impact into the solid massive target placed at the collider channel exit. In particular, they included: the interaction of the laser beam with the projectile ablator and the absorption of the laser radiation in the plasma produced and confined in the cavity, the shock generation in the projectile (by the plasma pressure) and its heating and acceleration in the guiding channel, the interaction of the projectile with the channel wall during the acceleration, the impact of the projectile into the massive target and the generation of the shock in the target and, finally, heating the target by the shock, melting and evaporating of the target material and, as a result, the formation of a crater in the target. The simulations of the acceleration phase were carried out in Lagrangian coordinates applying a mesh moving with the plasma. In turn, in the impact phase, the simulations were performed in the Eulerian coordinates with a static computational mesh as the computational domain in this phase does not change. In this phase, the computations had been conducted for a long time (typically, for ~ 1000 ns) up to the moment when parameters (pressure, temperature, velocity) of the shock, generated shortly after the impact and propagating in the target, became too low to melt the target material, and the dimensions of the crater produced as a result of vaporization and melting of the material stopped to increase. Both in the acceleration phase and the impact phase, the QEOS equations of state [26] were applied to describe thermodynamic properties of materials used in the projectile and the impacted targets. For both phases computations were performed in the cylindrical r, z geometry.

The simulations were performed for the same parameters of the LICPA-driven collider as the ones used in the experiment carried out recently at the PALS laser facility [20]. The cavity and the guiding channel walls were made of gold and the main collider dimensions were as follows: the cavity length $L_c = 0.4$ mm, the channel length $L_{ch} = 2$ mm, the cavity diameter $D_c = 0.3$ mm, and the channel diameter $D_{ch} = 0.3$ mm. As a projectile in its initial state we applied the gold disc of the thickness of 2.8 μm and the diameter of 0.3 mm (the projectile mass $m_p \approx 4$ μg), covered by the CH ablator of the thickness of 5 μm . The massive targets placed at the collider channel exit were made of Au, Cu, Al or CH. The laser beam parameters on the target (CH ablator) were assumed to be relevant to the parameters of the 3ω PALS laser beam, in particular: the laser wavelength $\lambda = 0.438$ μm , the pulse duration $\tau_L = 0.3$ ns, the transverse beam intensity distribution $\sim \exp(r/r_0)^6$ with $r_0 = 170$ μm . For the laser energy $E_L = 200$ J, these parameters correspond to the beam peak intensity on the target $\sim 10^{15}$ W/cm^2 . The laser beam energy varied within the range $10 - 400$ J.

The correctness and accuracy of the PALE code used for the simulations was verified for various laser-based schemes of shock generation [20,27,28], in particular for the LICPA-based collider [20]. Highly positive results of these verifications allow us to believe that numerical results obtained in this paper are correct not only qualitatively but also quantitatively within a factor ~ 1.5 or smaller.

Using the PALE code we examined how parameters and the structure of the shock generated in a massive target by the projectile impact are influenced by the properties of the target material and especially by the material density. Figure 1 presents 2D spatial distributions of the density and the pressure in the impacted target ($z < 0$) made of Au or CH at the moment $t = t_{\text{pmax}}$ when the pressure in the target attains the highest value. Although maximum values of these parameters in the generated shock significantly depend on the kind of the material, for all target materials used the spatial shape of the shock is similar – the shock is rather flat and homogeneous within $2r = 200 \mu\text{m}$. The quasi-planar shape of the shock is preserved up to ~ 1 ns after reaching by the shock the highest pressure, and after this period a radial expansion of the shock begins to be significant.

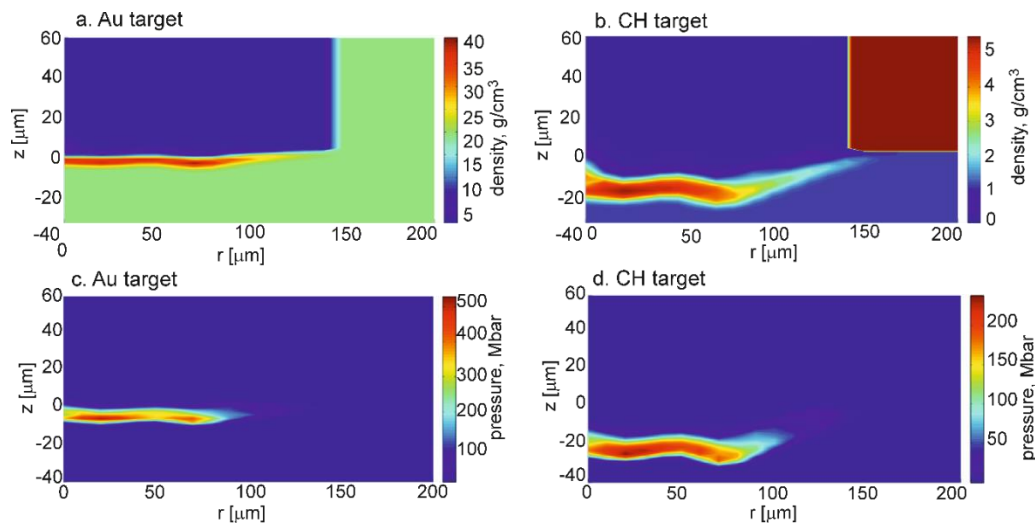


Figure 1. 2D spatial profiles of density (a, b) and pressure (c, d) inside targets ($z \leq 0$) made of Au or CH at the moment when the pressure in the target attains the highest value. The targets are impacted by the gold projectile accelerated in the collider channel situated in the region $z > 0$, $r < 150 \mu\text{m}$. $E_L = 200 \text{ J}$.

The highest value of pressure in the impacted target changes in time. The simulations showed that the maximum pressure (in the target space) attains its peak value very fast (within ~ 0.2 ns) independently of the target material. It indicates a very short time of energy transfer from the projectile to the target, which is a consequence of the high velocity and compactness (small effective thickness) of the projectile. However the “pressure pulse” duration depends on the target material and for the gold target the duration (FWHM) is by a factor ~ 1.5 shorter than for the plastic target. In the time period of $\Delta t = 1$ ns after the impact, when planarity of the shock is preserved, the maximum shock pressure averaged in time is by a factor $1.5 - 2$ lower than the peak pressure and lays in the sub-Gbar range for all the targets used in the simulations. This period is by a factor ~ 2 longer than that estimated for the sub-Gbar pressure range in the hyper-velocity impact experiment with the multi-kJ Nova laser [15] and seems to be long enough to measure some parameters of the material compressed by the shock, e.g. those required for the determination of equation of state of the material.

The summary of quantitative results of the simulation of shock generation by the projectile impact in the targets made of different materials are shown in figures 2, 3 and 4. Figure 2a presents the maximum (in space and time) pressures and velocities of the shocks attained in the targets and figure 2b the laser-to-shock energy conversion efficiency $\eta_{\text{ls}} = E_s/E_L$ for the time $t = t_{\text{pmax}}$ when the pressure reaches the highest value and for t equal to 5ns after the impact. The shock energy E_s is defined here as

the energy of the target material which is flowing along the axis z into the target interior with the velocity higher than $\frac{1}{4}$ of the maximum flow velocity. The maximum shock velocity decreases with an increase in the target material density while the maximum shock pressure increases with the material density and it approaches 500 Mbar for Au and Cu and surpasses 300 Mbar for Al. So far, such high values of the pressure could be produced with the laser-based methods only with the use of large multi-kJ lasers. Here, the sub-Gbar shock pressures are achieved at laser energy of only 200 J. Achieving such high pressures in the LICPA-driven collider at relatively small laser energy is possible thanks to the very high efficiency of the projectile acceleration by the LICPA mechanism, high efficiency of the energy transfer from the projectile to the target due to high projectile density and a short interaction time between the projectile and the target (being the result of compactness and high velocity of the projectile). The first two factors also determine the high value of the laser-to-shock energy conversion efficiency which for low-density targets (CH, Al) approaches 20 % and is by an order of magnitude higher than the efficiencies attained with laser-based methods so far.

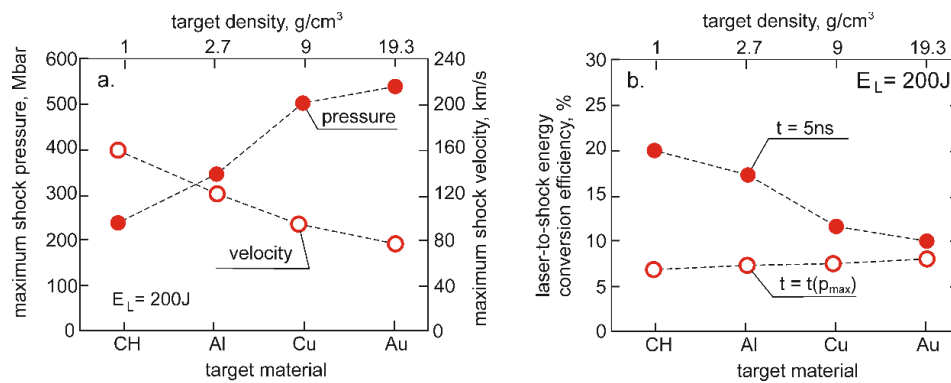


Figure 2. The maximum values of pressure and velocity of the shock generated inside the targets made of various materials impacted by the gold projectile (a). The laser-to-shock energy conversion efficiency for the targets made of various materials at the moment $t = t_{p_{\max}}$ when the shock pressure achieves the highest value and at the moment of 5 ns after the gold projectile impact (b). $E_L = 200$ J.

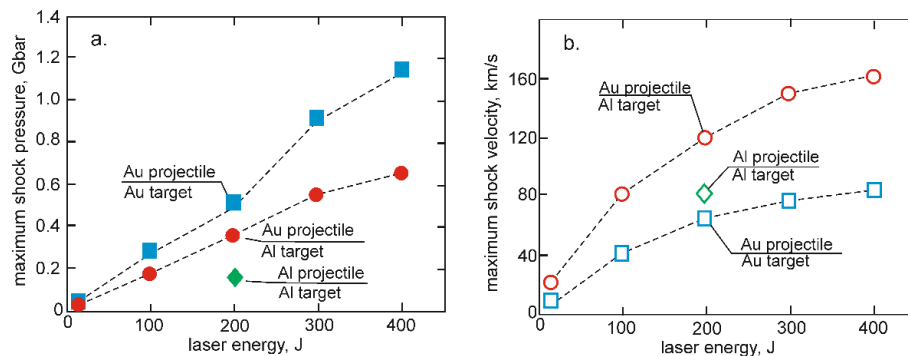


Figure 3. The maximum values of pressure (a) and velocity (b) of the shock generated inside the Au (squares) and Al (circles) targets impacted by the gold projectile as a function of laser energy. The diamonds corresponds to the case when the Al target is impacted by the aluminum projectile of the mass equal to the mass of the gold projectile.

The dependencies of the maximum (in space and time) pressure and velocity of the shocks generated in the Al and Au massive targets by the gold projectile accelerated in the LICPA-based collider, for the energy range of 10 – 400 J accessible at the PALS facility, are presented in figure 3. The shock pressure increases almost linearly with the laser energy for both targets and at $E_L = 400$ J it attains 0.7 Gbar for Al and near 1.2 Gbar for Au. The shock velocity increases approximately as $E_L^{1/2}$ with an increase in the laser energy and for $E_L = 400$ J it reaches 160 km/s for Al and about 80 km/s

for Au. In the figure, there is also presented the maximum pressure and velocity of the shock generated in the Al massive target by the Al projectile of the same mass (and areal density) as that of the Au projectile and driven by the laser energy of 200 J. It can be seen that the maximum pressure and the maximum velocity of the shock generated by the gold projectile are greater by a factor of ~ 2 and ~ 1.5 , respectively, than those of the shock produced by the Al projectile. The main reasons for the observed difference in the shock parameters are higher density (by a factor $\sim 3 - 4$) and smaller thickness of the impacting gold projectile as compared to the Al projectile which allows for the transfer of the gold projectile energy to the impacted target with higher efficiency and during a shorter time than in the case of the Al target.

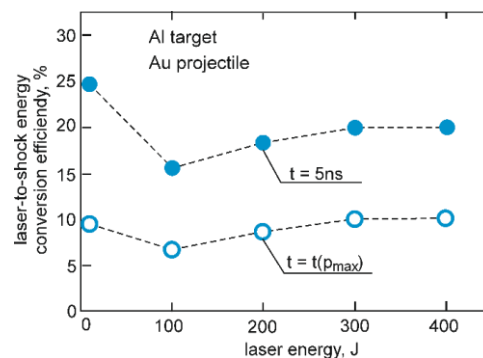


Figure 4. The dependence of the laser-to-shock energy conversion efficiency in the Al target impacted by the gold projectile on the laser energy for the moment when the shock pressure reaches the highest value (open circles) and for the moment of 5 ns after the impact (full circles).

The laser-to-shock energy conversion efficiency, η_{ls} , as a function of the laser energy, for the Al massive target and two moments after the gold projectile impact, is presented in figure 4. The conversion efficiency decreases with an increase in the laser energy in the low energy range (below of 100 J) and then slightly increases. At $E_L = 400$ J, the conversion efficiency reaches 10% at the early phase of the shock formation (when the shock pressure reaches the maximum value) and 20% in the late phase (at $t = 5\text{ ns}$). Qualitatively similar dependence of the conversion efficiency on the laser energy was observed for the Au target; however, in this case the conversion efficiency in the high energy range was $< 15\%$.

3. Conclusions

In conclusions, the production of high-pressure shocks in solid targets using the hyper-velocity impact in the recently proposed LICPA-driven collider has been investigated using hydrodynamic simulations. It has been found that with the laser driver energy of only a few hundred joules, sub-Gbar-pressure shocks can be generated in the collider with the laser-to-shock energy conversion efficiency by an order of magnitude higher than in other laser-based schemes used so far. The peak pressure of the shock depends on both the projectile density and the impacted target density and it increases with an increase in these densities. In the laser energy range of 10 – 400 J, the peak pressure approximately linearly increases with the laser energy. The laser-to-shock energy conversion efficiency relatively weakly depends on the laser energy; however, it significantly depends on the target density – for a gold projectile driven by the laser pulse of energy of 200 J it reaches $\sim 10\%$ for the Au target and $\sim 20\%$ for the CH target. For all the target applied (Au, Cu, Al, CH) the pressure in the shock increases to its peak value very rapidly (within $\Delta t < 0.3\text{ ns}$ for $E_L = 200\text{ J}$) and for the time period of $\Delta t = 1\text{ ns}$ after the impact, when planarity of the shock is preserved, the maximum shock pressure averaged in time lays in the sub-Gbar range both for the high-density and low-density targets used in the simulations. The results presented in the paper suggest that the LICPA-driven collider can be an efficient tool for the shock generation both in case of laser energies higher than those considered in the paper ($\sim 1\text{ kJ}$ or higher) and in case of low laser energies ($\sim 5 - 10\text{ J}$) produced by

commercial lasers. The last possibility would open a prospect for conducting research in high energy-density science also in small, university-class laboratories.

Acknowledgments

This work was supported in part by the Ministry of Science and Higher Education, Poland under the grant no W39/7.PR/2015. Also, this work was supported in part by the Czech Ministry of Education, Youth and Sport, projects LD 14089 and RVO 68407700, as well as by the Eurofusion Consortium, project AWP15-ENR-01/CEA-02.

4. References

- [1] Drake RP 2006 *High-Energy-Density Physics* (Springer, Berlin).
- [2] Nellis W J 2016 *Rep. Prog. Phys.* **69**,1479.
- [3] Kraus D, Ravasio A, Gauthier M, et al. 2016 *Nat. Comm.* **7**, 10970.
- [4] Atzeni S and Meyer-ter-Vehn J, 2004 *The Physics of Inertial Fusion* (Clarendon, Oxford).
- [5] Fortov V E 1982 *Sov. Phys. Usp.* **25**, 781.
- [6] Trunin R F 1994 *Phys. – Usp.* **37**, 1123.
- [7] Veeseer L R and Solem S C 1978 *Phys. Rev. Lett.* **40**, 1391.
- [8] Batani D, Morelli A, Tomasini M, et al. 2002 *Phys. Rev. Lett.* **88**, 235502.
- [9] Gus'kov S Yu., Kasperczyk A, Pisarczyk T, et al. 2007 *J. Exp. Theor. Phys.* **105**, 793.
- [10] Batani D, Antonelli L, Atzeni S, et al. 2014 *Phys. Plasmas* **21**, 032710.
- [11] Löwer Th, Sigel R, Eidmann K, et al. 1994 *Phys. Rev. Lett.* **72**, 3186.
- [12] Lemke R W, Knudson M D, Bliss D E, et al. 2005 *J. Appl. Phys.* **98**, 073530.
- [13] Mitchell A C, Nellis W J, Mariorty J A, et al. 1991 *J. Appl. Phys.* **69**, 2981.
- [14] Obenschain S P, Whitlock R R, McLean E A, et al. 1983 *Phys. Rev. Lett.* **50**, 44.
- [15] Cauble R, Phillion D W, Hoover T J, et al. 1993 *Phys. Rev. Lett.* **70**, 2102.
- [16] Karasik M, Weaver J L, Aglitskiy Y, et al. 2010 *Phys. Plasmas* **17**, 056317.
- [17] Frantaduono D E, Smith R F, Boehly T R, et al. 2012 *Rev. Sci. Instrum.* **83**, 073504.
- [18] Shui Min, Chu Gen-Bai, Xin Jian-Ting, et al. 2015 *Chin. Phys.* **B24**, 094701.
- [19] Min Shui, Genbai Chu, Bin Zhu, et al. 2016 *J. Appl. Phys.* **119**, 035903.
- [20] Badziak J, Rosiński M, Krousky E, et al. 2015 *Phys. Plasmas* **22**, 032709.
- [21] Badziak J, Krousky E, Kucharik M, and Liska R, 2016 *J. Instrum.* **11**, C03043.
- [22] Badziak J, Borodziuk S, Pisarczyk T, et al. 2010 *Appl. Phys. Lett.* **96**, 251502.
- [23] Badziak J, Jabłoński S, Pisarczyk T, et al. 2012 *Phys. Plasmas*, **19**, 053105.
- [24] Liska R, Kucharik M, Limpouch J, et al. 2011, in Fort J, et al., editors, *Finite Volumes for Complex Applications VI, Problemes & Perspectives*. Vol. 2 p. 57-73, Springer-Verlag.
- [25] Kapin T, Kucharik M, Limpouch J, et al. 2008 *Int. J. Numer. Methods Fluids* **56**, 1337.
- [26] More R M, Warren K H, Young D A and Zimmerman G B 1988 *Phys. Fluids* **31**, 3059.
- [27] Koester P, Antonelli L, Atzeni S, et al. 2013 *Plasma Phys. Control. Fusion* **55**, 124045.
- [28] Badziak J, Antonelli L, Batani D, et al. 2015 *Laser Part. Beams* **33**, 561.